Student thesis series INES nr 569

Tundra carbon cycling in relation to sea-ice decline in a warming Arctic

Juliane Glinski

2022
Department of
Physical Geography and Ecosystem Science
Lund University
Sölvegatan 12
S-223 62 Lund
Sweden

Juliane Glinski (2022).
Tundra carbon cycling in relation to sea-ice decline in a warming Arctic
Bachelor degree thesis, 15 credits in Physical Geography and Ecosystem Analysis
Department of Physical Geography and Ecosystem Science, Lund University

Level: Bachelor of Science (BSc)

Course duration: *January* 2022 until *June* 2022

Disclaimer

Tundra carbon cycling in relation to sea-ice decline in a warming Arctic

---

Juliane Glinski

Bachelor thesis, 15 credits, in Physical Geography and Ecosystem Analysis

Supervisors:
Frans-Jan Parmentier
University of Oslo
Lund University

Alexandra Pongracz
Lund University

Exam committee:
Hans Chen, Lund University
Marko Scholze, Lund University

Acknowledgements

I would like to express thanks to my supervisor Frans-Jan Parmentier and Alexandra Pongracz who equipped me with the data, helped me find my way and gave me feedback which improved my paper a lot.

Special thanks go to my partner Thanh-Van and to my friend Cole, who both helped me solve some tricky programming issues.

Thanks go to my family as well who support me in everything I do and provide me with the opportunity to study in Sweden.

Abstract

We set out to investigate whether arctic tundra acted as a sink or source of carbon dioxide (CO_2) between 1980-2014 and to relate changes in the net carbon balance to Arctic sea-ice decline. We want to understand how climate change and arctic warming influence arctic carbon cycling. Identifying the ways higher temperatures affect tundra carbon cycling, one of them being the decline of sea ice, can deepen the understanding we have of climate change.
Trends in arctic tundra Net Ecosystem Exchange (NEE) over 1980-2014 were investigated and related to changes in sea-ice area and temperature. We analyzed the changes in modelled NEE in relation to sea-ice decline and increasing temperatures by looking at trends in simulated Gross Primary Production (GPP), autotrophic respiration (RA) and heterotrophic respiration (RH). These were correlated with sea-ice area and temperature data. Carbon fluxes were modelled by a customized arctic version of the LPJ-GUESS dynamic global vegetation model.

NEE became more negative over 1980-2014, indicating an increase in the carbon sink of tundra (GPP). Also, auto- and heterotrophic respiration increased with warming temperatures and sea-ice decline, agreeing with previous work that a warming Arctic facilitates tundra productivity. The increases in GPP, RA and RH were found to be significantly related to the decreases in sea-ice area and temperature increases. Seasonal investigations revealed that GPP was affected the least by temperature in autumn and winter. This causes the typical variations in NEE over the year, varying from negative (sink of carbon) to positive (source of carbon) values. The CO_2 flux of GPP increased between the first and last 10 years investigated (1980-1989 and 2005-2014), by an average of 762 TgC y^{-1}. CO_2 from ecosystem respiration increased by an average of 605 $TgCyr^{-1}$ and NEE decreased by 157 $TgCyr^{-1}$. Our finding of an increasingly negative NEE from 1980 to 2014 shows that the increased carbon losses through RA and RH were compensated by an increasing carbon sink through GPP and that this sink increased with sea-ice decline and arctic warming.

Keywords: sea-ice decline, warming Arctic, earlier growing season, arctic tundra, heterotrophic and autotrophic respiration, climate warming

Table of Contents

Abbreviations

LPJ-GUESS – Lund-Potsdam-Jena General Ecosystem Simulator

GPP – Gross Primary Production: measure of photosynthetic activity

RA – Autotrophic respiration: respiration by live roots and plant metabolic processes

RH – Heterotrophic respiration: respiration from the decomposition of soil organic matter (SOM) and plant residues by soil microbes

R_{eco} – Ecosystem respiration: sum of carbon respired by the ecosystem (RA+RH)

NDVI – normalized difference vegetation index: a proxy for live biomass

NEE – Net Ecosystem Exchange: measure of the net exchange of carbon between an ecosystem and the atmosphere

PFT – Plant Functional Type: plant classification system used in vegetation models

SAT – Surface Air Temperature

1 Introduction

Climate change is occurring twice as fast in the Arctic compared to the rest of the world, with an annual average temperature increase of 2.7 °C in 2017 compared to 1971 (Box et al., 2019). Such a strong temperature increase has large consequences on Arctic systems, such as the decline of sea ice (Box et al., 2019). Extensive and rapid losses in sea-ice area since 1979 (Moon, 2021) are one of the most profound examples of climate change (Parmentier et al., 2013). This retreat of sea ice results in a lower surface albedo and a higher absorption of solar energy, which further warms the Arctic, feeding into more losses of sea ice. This feedback process is one of the main causes of the pronounced warming in the polar region, also known as *Arctic amplification* (Box et al., 2019).

The causal relationship between temperature increases and sea-ice decline is widely established (Box et al., 2019; Parmentier et al., 2013), however, the effects of the marine changes on terrestrial carbon fluxes is less often investigated. It is unclear how strong the influence of temperature change through sea-ice decline is on Net Ecosystem Exchange (NEE), the net balance between carbon uptake and emission.
Earlier snowmelt in spring, and longer snow-free periods resulting from the strong warming, are key influences on plant growth and the carbon cycling of terrestrial vegetation (Box et al., 2019). Increases in temperature allow for higher biomass production, which means that the productivity of tundra vegetation can be promoted through warming from sea-ice decline. This is supported by observations of increased normalized difference vegetation index (NDVI) (Bhatt et al., 2017), indicating higher photosynthetic activity (Demura & Ye, 2010). Indeed, observations of a more active carbon cycle with higher plant productivity but also higher plant respiration, especially at the end of the warm season, have been reported (Bruhwiler et al., 2021). Another result of warmer temperatures in tundra ecosystems is the thawing of permafrost. The resulting higher substrate availability, and further warming of the soil, promote microbial activity, higher decomposition rates and the bioavailability of previously stored carbon that can be released in the form of heterotrophic respiration (Pongracz et al., 2021). This raises the question on whether gross primary production (GPP) or auto- and heterotrophic respiration (RA and RH) will be the dominant carbon flux under climate change.

It is critical to understand the effects of sea-ice decline on the carbon cycling of tundra, as resulting changes in tundra productivity and vegetation composition can further alter the atmospheric balance of carbon and energy exchange, and ultimately feed back to changes in temperature and sea-ice area (Buchwal et al., 2020). The high availability of sunlight during spring allows for an increase in GPP when sea-ice melt leads to higher temperatures and earlier snowmelt (Parmentier et al., 2013). However, the warming effect from sea-ice decline is strongest in autumn and early winter (Screen et al., 2012), when sunlight is limited and therefore GPP may not increase as much, whereas respiration rates can rise regardless of the season (Parmentier et al., 2013).

Part of the problem is the high uncertainty on the size of the terrestrial carbon budget of the high latitudes (Virkkala et al., 2021), especially for those of high latitude tundra and boreal biomes (López-Blanco et al., 2019; Schuur et al., 2015; Zscheischler et al., 2017). Regional estimates of the tundra carbon balance based on measurements vary from sinks (McGuire et al. 2012; Virkkala et al., 2021) to sources (Belshe et al., 2013). The large uncertainty in observational records due to data gaps across the Arctic-Boreal region suggests the use of models to look at how ecosystems may respond to warming.

Parmentier et al. (2013) point to the need for further investigation on the impact of temperature (and longer growing seasons) on plant productivity and NEE through surface measurements and modelling. Modelled data avoids the dependence on the availability of measured datasets. It allows for continuous analysis through time, as well as for estimations of respiration, compared to data from satellite measurements, as used in previous studies (Parmentier et al., 2013).

This paper aims to investigate the relationship between changes in sea-ice area and fluxes of terrestrial carbon, looking at GPP, NEE, RA and RH, as well as to determine how long-term temperature trends link to this relationship. The following work looks at sea-ice area and surface temperature from climate forcing data to determine the effect sea-ice decline and arctic warming had on the carbon cycling of arctic tundra over the period 1980-2014.

1.1 Aims and objectives

The modelled and observational data will be used to investigate

- whether arctic tundra acted as a sink or source of carbon between 1980-2014
- the trends in sea-ice area, temperature and carbon exchange
- how sea-ice decline and increasing temperatures link to changes in tundra carbon cycling
- and to quantify these fluxes in GPP, RA, RH and NEE

1.2 Hypotheses

1) We expect to see a positive trend in temperature and a negative trend in sea-ice area, as shown previously (Box et al., 2019), which in turn may lead to positive trends in GPP and respiration.
2) With a warming Arctic we expect to see a positive trend in tundra NEE over 1980-2014, due to a stronger increase in the release of CO_2 through ecosystem respiration (R_{eco}) than the uptake of CO_2 through photosynthesis (GPP).
3) We expect that a significant negative relationship ($p < 0.05$) exists between sea-ice area and GPP as well as between sea-ice area and respiration, i.e., as sea ice melts, photosynthesis and respiration will occur at higher rates.
4) We further expect that GPP will be less raised and affected by temperature during autumn and winter due to the unavailability of light for photosynthesis compared to respiration which can occur over a longer period of the year.

2 Material and Methods

We followed the methodology first shown by Parmentier et al. (2013) for a link between sea-ice decline and methane emissions. This new analysis uses, besides sea-ice satellite data, modelled CO_2 fluxes and climate forcing data which improves upon previous analyses (Parmentier et al., 2013) by looking at links between sea-ice decline and GPP and respiration.

The study area includes sea ice and tundra north of 60° latitude. Rising surface air temperatures (SAT) between 1990-2008 were found to be strongest in the Arctic maritime region (Polyakov et al., 2012), mainly occupied by the tundra biome, therefore most likely affected by changes in sea-ice area and resulting SAT changes.

This study uses a model run from a customised Arctic version of LPJ-GUESS (version 4.0, subversion 10384) that simulated NEE, GPP, RA and RH. We only consider vertical CO_2 exchange and not methane, since CO_2 fluxes form the majority of the arctic carbon budget (Bruhwiler et al., 2021). The model was forced with CRUNCEP version 7 monthly atmospheric forcing data including air temperature, precipitation and incoming solar radiation. This dataset is a compilation of the dataset CRU TS3.2 (0.5 °resolution) covering the period 1901-2002 and the NCEP reanalysis of 2.5° resolution with 6-hourly data for 1948-2016, merged into the global reanalysis climate dataset CRUNCEP version 7 (Pongracz et al., 2021; Viovy, 2018). This dataset was also used for our atmospheric analyses.

Furthermore, monthly mean sea-ice concentration between October 1978 through August 2021 was used (Comiso 2017). This dataset is collected by the satellite sensors SSM/I, SMMR and SSMIS, which cover the entire globe, except for a circular gap near the North Pole due to the orbital inclination of older satellites. The spatial resolution of the data varies from 27 km at 37 GHz to 148 km at 6.6 GHz. The data is gridded on the SSM/I polar stereographic grid (25 x 25 km). Sea-ice concentrations were derived from the revised Bootstrap algorithm (Comiso 2017). To be able to perform correlations between these variables, all datasets were sliced to the period 1980-2014.

2.1 LPJ-GUESS

LPJ-GUESS (Smith et al., 2001; Smith et al., 2014) is a process-based dynamic global vegetation model used for regional and global vegetation simulations (Pongracz et al., 2021; Smith et al., 2001; Smith et al., 2014). The model acts on an individual and patch scale, taking into account growth, competition for resources, as well as disturbances and resulting vegetation composition and distribution in the ecosystem. The model represents vegetation-, soil nitrogen, and plant dynamics and their limits on plant productivity and the terrestrial carbon balance (Smith, 2001; Smith et al., 2014) (see *Figure 2*).

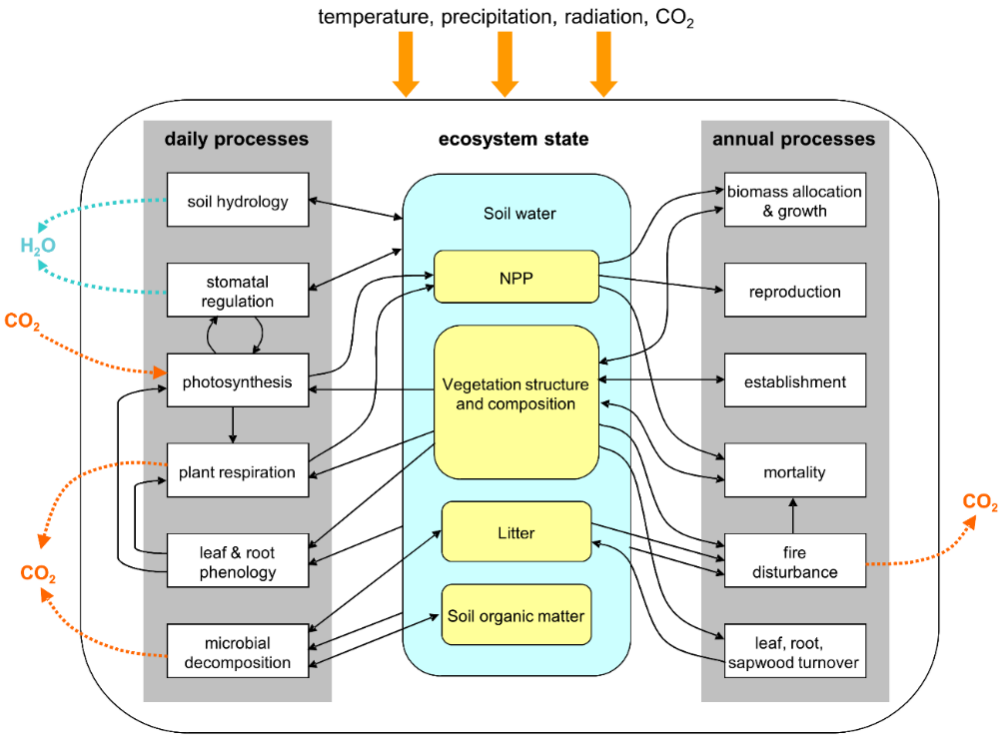

Figure 1. Schematic overview of the processes in LPJ-GUESS. Figure taken from Smith (2001).

This version of LPJ-GUESS contains an updated dynamic snow-scheme developed by Pongracz et al. (2021) which models snow and permafrost more advanced and enables a more precise modelling of carbon fluxes in winter, which are often underestimated in models (Pongracz et al., 2021). 15 plant functional types (PFTs) are used in the model to represent arctic-boreal vegetation, as shown in *Table 1* below:

Table 1. Plant functional types (PFTs) used for the Arctic version of LPJ-GUESS. BNE and BINE differ in their shade tolerance. Table taken from Pongracz et al., (2021).

PFT	Description	Vegetation group
BNE	Boreal needleleaved evergreen tree	forest
BINE	Boreal needleleaved evergreen tree	forest
BNS	Boreal needleleaved summergreen tree	forest
IBS	Shade-intolerant broadleaved summergreen tree	forest
TeBS	Shade-tolerant temperate broadleaved summergreen tree	forest
HSE	Tall shrub, evergreen	shrub
HSS	Tall shrub, summergreen	shrub
LSE	Low shrub, evergreen	shrub
LSS	Low shrub, summergreen	shrub
GRT	Graminoid and forb tundra	grass
EPDS	Prostate dwarf shrubs (needleleaved, evergreen)	grass
SPDS	Prostate dwarf shrubs (broadleaved, summergreen)	grass
CLM	Cushion forb, lichen and moss tundra	grass
C3G	C3 grass	grass

We focus on the modelled carbon fluxes of NEE, GPP, RA and RH. We look at RA and RH separately and also calculate R_{eco} (sum of RA and RH). This is done to see whether they are differently influenced by a warming climate and declining sea-ice.

The simulated carbon flux outputs NEE, GPP, RA, RH and ecosystem respiration (R_{eco}) can be put into relation to each other with the following equations:

$$NEE = -GPP + Reco$$

where

$$Reco = RA + RH$$

GPP is a measure of the fixation of CO_2 by plants through photosynthesis and is here defined as a positive flux, as well as autotrophic respiration (plant respiration) and heterotrophic respiration (what is respired by soil microbes). NEE shows the net exchange of carbon of arctic tundra with the atmosphere in this study. If tundra releases more carbon through respiration than it takes up through photosynthesis, NEE is positive and vice versa.
Figure 1 shows the processes simulated in a terrestrial biosphere model like the Lund–Potsdam–Jena General Ecosystem Simulator (LPJ-GUESS). LPJ-GUESS simulates vegetation dynamics, carbon fluxes and water dynamics, which are controlled by solar radiation, air temperature and precipitation. Many processes are involved in the exchange of terrestrial carbon (see *Figure 1*). Here we focus on GPP and R_{eco}, the most important fluxes governing net ecosystem exchange of CO2.

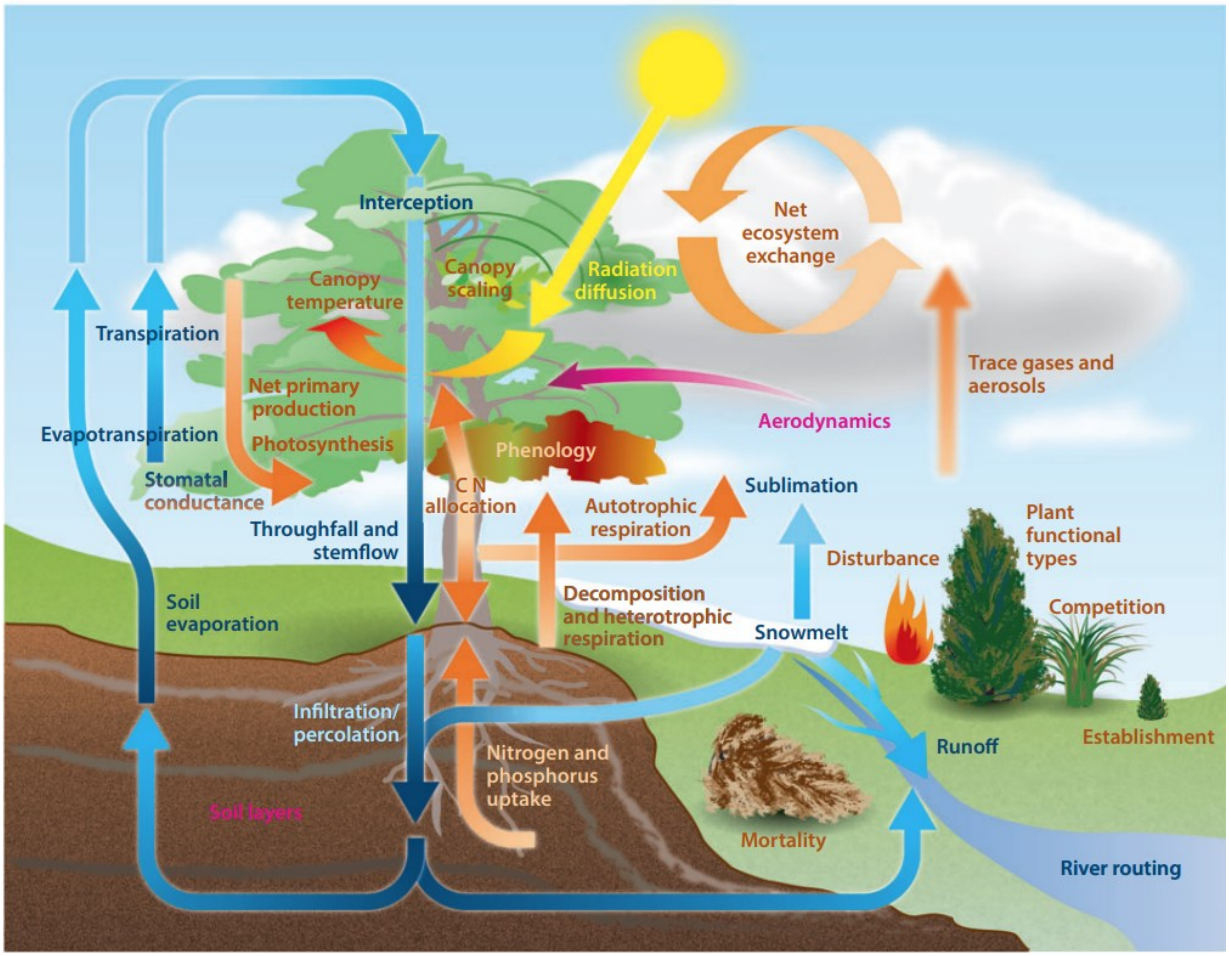

Figure 2. The processes simulated in a terrestrial biosphere model such as LPJ-GUESS. Figure taken from Fisher et al. (2014). When tundra acts as a net source of carbon to the atmosphere, the value for NEE will be positive, whilst an overall sink of carbon will be indicated by a negative value.

2.2 Data processing

Data processing was done in Python (3.1.0) and Microsoft Excel. The following modules and packages were used in Python: netCDF4 (Unidata, 2012), NumPy (Harris et al., 2020), pandas (McKinney, 2010, 2015) and xarray (Hoyer & Hamman, 2017).

2.2.1 **Closing the polar hole data gap**

Sea ice fraction contains no data at the polar region above 84.5° for SMMR and 87.2° N for SSM/I and SSMIS. This is due to the orbital inclination of those satellites and the reason for the circular hole. This region is commonly assumed to have had full ice coverage during the times of data acquisition (Meier et al., 2008) and therefore sea-ice fraction was set to 1 (representing a coverage of 100%).

2.2.2 **Calculating total sea-ice area**

Our definition of sea-ice area in this study is as follows. We consider all pixels regardless of percentage of ice cover including pixels containing less than 15% ice. Total sea-ice area in millions of square kilometres (north of 60°) was calculated by multiplying the variables sea-ice fraction (the actual fraction from 0% to 100% ice coverage) with grid cell area. The area was sliced to the years 1980-2014 and averaged per season for the time span 1980-2014. Seasonal data was selected for the months 'MAM' (March, April and May for spring), 'JJA' (June, July

and August for summer), 'SON' (September, October and November for autumn) and 'DJF' (December, January and February for winter).

2.2.3 **Quantification of carbon fluxes**

A similar method was applied to the carbon flux data, although for this data, a mask was used (see *Figure 3*) to filter out areas not occupied by tundra vegetation. This mask separates the dataset in two categories: tundra and not-tundra. For the purpose of this study, we assume that tundra is the most affected by sea-ice induced warming. Tundra is situated closer to the Arctic Ocean and thus more likely to be affected by changes in sea-ice concentration and resulting temperature changes than boreal forest (Polyakov et al., 2012). All carbon fluxes were summed over each season and multiplied by the grid cell area.

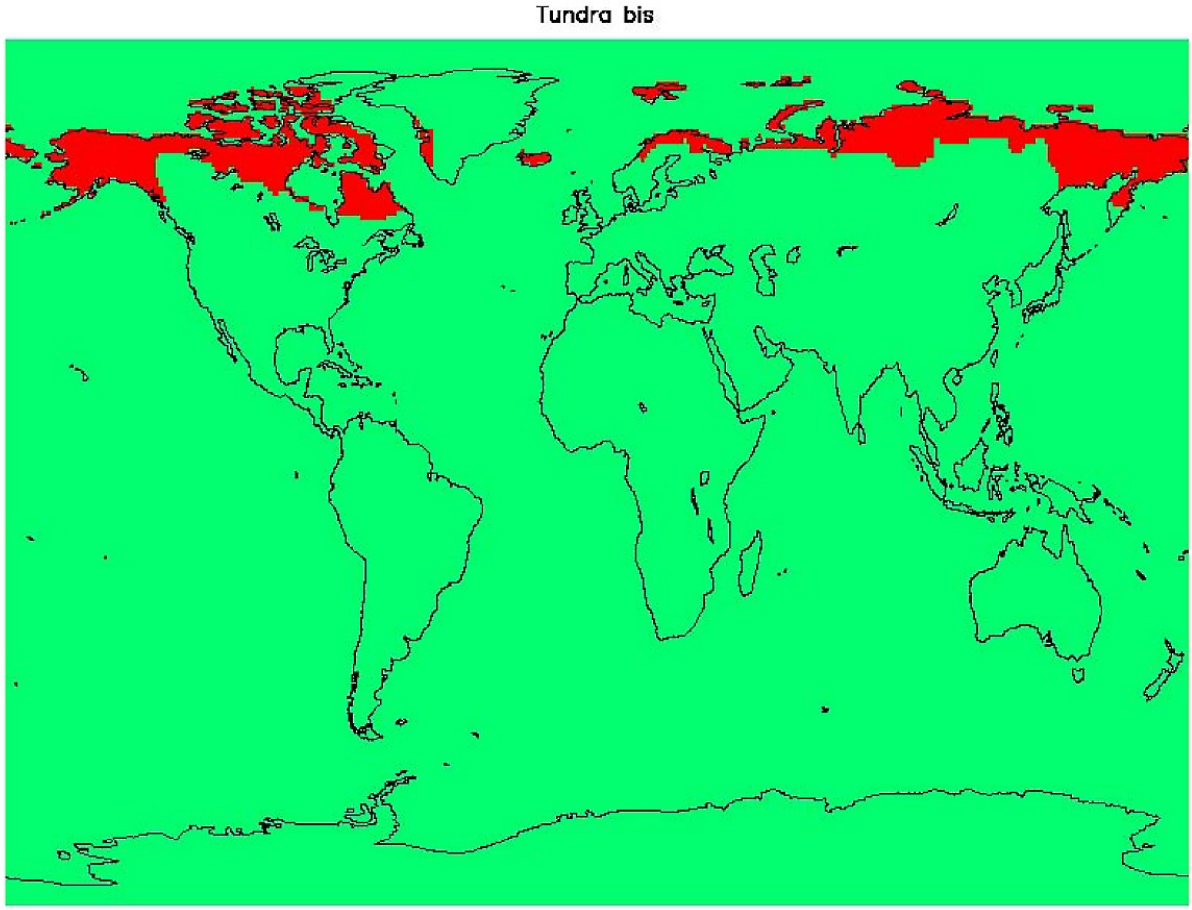

Figure 3. Tundra mask taken from McGuire et al. (2012). Red regions represent the tundra region as used in this study.

2.2.4 **Extracting tundra temperature data**

The same method as in section 2.2.4 was applied to the temperature data, except that it was not summed but averaged over each season (see section 2.2.3 for detail on the seasons). This gives mean seasonal temperatures for tundra over the timespan 1980-2014.

2.3 Data analysis

2.3.1 **Temporal trends and variations**

Annual and seasonal average changes in carbon fluxes between the first and the last 10 studied years were calculated. This smooths out the interannual variability. Carbon trends were plotted per season to uncover seasonal variations and to compare how each variable varied over the

years. Graphs comparing total sea-ice area with average temperature trends and total trends in GPP, NEE, RA and RH were created per season. To test whether the linear trend for the carbon fluxes was significantly different from 0 the probability value (p-value) of these trends was calculated (two-sided probability), for which the statistical significance level was set to $\alpha < 0.05$ for the 35 sample years.

2.3.2 **Correlations**

Correlations were performed in Microsoft Excel. To avoid strong correlations due to unrelated long-term linear trends in both variables, all exported seasonal data were linearly detrended following Parmentier et al. (2015). This shifts the focus to the interannual variability, while spurious correlations due to the same underlying long-term factor are removed, such as background global warming. The detrended data of sea-ice area were then correlated with the detrended temperature, GPP, NEE, RA and RH data. Correlations were also performed between temperature and each of the carbon fluxes. Significance of a correlation was as in section 2.3.1 determined through the probability value p (two-sided probability). Significance is defined as $p < 0.05$, which for the length of our time series meant that correlations larger than 0.34 ($r > 0.34$) are significant.

3 Results

3.1 Temporal trends

3.1.1 **Quantification of carbon fluxes**

Figure 4 shows the trend in NEE over all years, where NEE is expressed as a sum of total CO_2 exchanged (TgC y^{-1}). In contrast to our second hypothesis, NEE was found to have been negative throughout the years 1980-2014, with a negative trend. A significance test revealed that the trends in NEE, GPP, RH and RA were significantly different from 0 ($p<0.05$) (H0: there is no long-term linear trend in the data, and H1: there is a long-term linear trend), indicating that these trends are statistically significant at the $\alpha = 0.05$ level, meaning that a linear model describes the long-term changes in the carbon data well .

Total numbers of GPP, respiration and NEE are given in *Table 2*. During the first studied 10 years (1980-1989) GPP, as well as respiration, were lower than during the last 10 years (2005-2014): increases of 762 TgC y^{-1} and 605 TgCy^{-1}, for GPP and R_{eco} respectively. RH was higher than RA, however, RA increased more (+ 323 TgC y^{-1}/ +30.6%) compared to RH (+282 TgC y^{-1}/ +16.3%). NEE was less negative -197 TgC y^{-1}) between 1980-1989 than between 2005-2014 (-353 TgC y^{-1}). This gives a decrease in NEE by 156 TgC y^{-1} between the first and last 10 studied years.

Table 2. Average carbon fluxes during the first 10 and last 10 studied years and the difference between the averages. The relative difference is calculated by subtracting the first 10-year value from the last 10-year value and dividing this by the first 10-year value.

	GPP	RA	RH	R_{eco}	NEE
First 10 years (1980-1989) (TgC y^{-1})	2760	1058	1503	2561	-197
Last 10 years (2005-2014) (TgC y^{-1})	3522	1382	1785	3167	-353
Absolute Difference (TgC y^{-1})	+ 762	+ 323	+282	+605	-156
Relative difference (%)	+27.6	+30.6	+16.3	+23.6	-79.2

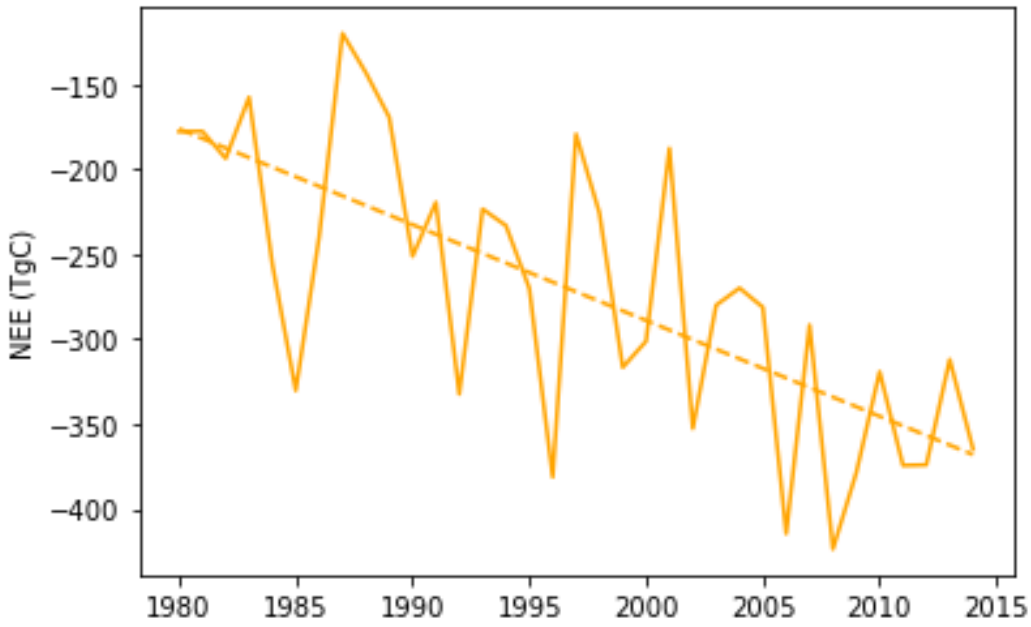

Figure 4. Interannual variations (gradient line) of NEE over 1980-2014 and the trend (dashed line).

3.1.2 **Seasonal trends in sea-ice area, temperature and carbon**

The changes in total GPP, respiration and NEE between the first and last studied 10 years are shown in *Table 2,* as well as the observed negative trend in NEE over the time period. These numbers, however, do not allow to identify the potential causes behind these changes. Therefore, we will now look at the seasonal variability. *Figure 5* shows the interannual variability in the seasonal fluxes and the trends in GPP, RA, RH and NEE

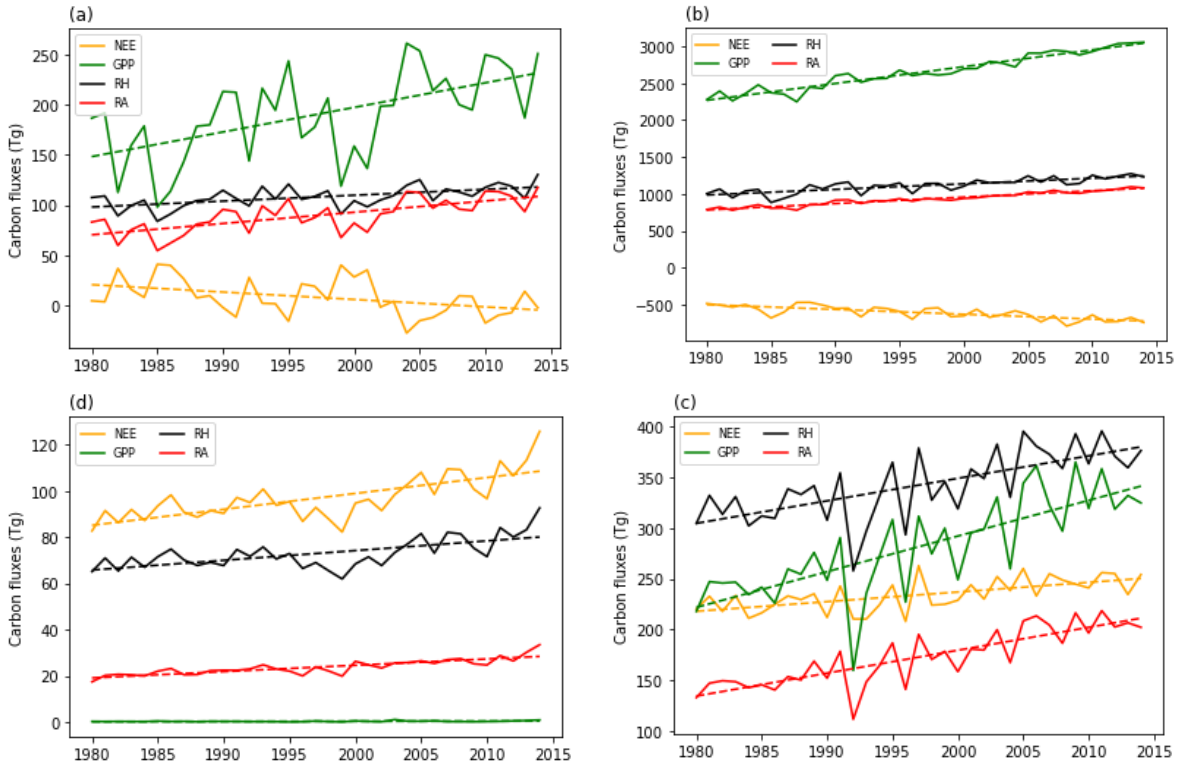

Figure 5. The interannual variations in GPP (green), RH (black), RA (red) and NEE (yellow) fluxes in TgC from 1980 to 2014: a) spring, b) summer, c) autumn and d) winter. Dashed lines represent the trend in each carbon flux.

GPP shows a positive trend during spring, summer and autumn, whilst there is no trend visible for winter GPP due to the lack of sunlight for photosynthesis. *Table 3* shows that GPP increased during all seasons between the first 10 and last 10 years (1980-1989 and 2005-2014), although only by 0.15 TgC during winter. This increase is most dominant for the summer (+600.88 TgC) and autumn period (+89.61 TgC), whilst spring GPP increased by 71.43 TgC.

Both heterotrophic and autotrophic respiration show a positive trend during all seasons (see *Figure 5*). Total changes in RA and RH can be seen in *Table 3*. As is the case for GPP, the highest increases in ecosystem respiration occurred during summer and autumn with 426.53 TgC y^{-1} for summer and 112.35 TgC y^{-1} for autumn. Winter ecosystem respiration increased at a much higher rate (+17.98 TgC y^{-1}) than winter GPP.
As can be seen from the seasonal NEE trends in *Figure 5*, respiration exceeded GPP in autumn and winter, whereas in spring and summer GPP is the stronger flux.

While heterotrophic and autotrophic respiration show similar patterns, autotrophic respiration was, according to our data, always lower than heterotrophic respiration (see *Figure 5*). The total increases in autotrophic respiration, however, were stronger than those in heterotrophic respiration during spring and summer, i.e., the proportional contribution of autotrophic respiration to ecosystem respiration increased in spring and summer. The difference between the two fluxes is larger during summer and autumn (see *Figure 4*).

The strongest warming between the first and the last 10 studied years occurred during spring and autumn by 0.58°C and 0.55°C, respectively. Sea-ice area decreased most during autumn and summer by -1.92 million km^2 and -1.83 million km^2 (See *Table 3*).

Table 3. Changes (increases and decreases) in temperature, sea-ice area, GPP, RA and RH between the average of the first 10 and the last 10 studied years (1980-1989 and 2005-2014).

	Spring	**Summer**	**Autumn**	**Winter**
Temperature (°C)	0.58	0.30	0.55	0.38
Sea-ice area (million km^2)	-0.91	-1.83	-1.92	-1.19
GPP (TgC y^{-1})	71.43	600.88	89.35	0.15
RA (TgC y^{-1})	31.53	227.45	57.61	6.78
RH (TgC y^{-1})	16.86	199.08	54.74	11.19
R_{eco} (TgC y^{-1})	48.39	426.53	112.35	17.98

NEE was negative for the summer period 1980-2014, positive in autumn and winter and fluctuated around zero during spring. A general decrease in NEE over time can be seen for spring and summer. A positive trend, on the other hand, was found for autumn and winter. The interannual variability is to be considered, as spring NEE fluctuates around zero, between positive and negative. The spring trend in NEE is towards zero.

The divergent response of NEE between the first and second half of the year can be explained by looking at the components that make up this flux: *GPP* and R_{eco}. In contrast to NEE, trends in GPP and R_{eco} were positive. Looking at the changes over time (see *Figure5)*, it becomes clear that for the seasons when GPP is higher than respiration, NEE shows a negative trend (summer) and when respiration dominates, the trend in NEE is positive (winter). During spring and autumn, the trend in NEE is weaker, when the variation over time in respiration and GPP is less pronounced.

In *Figure 6*, we compare these trends in NEE with the trends in total sea-ice area and temperature. A clear downward trend in sea-ice area and an upward trend in temperature occurred over the 35 studied years. As sea-ice declined and temperature increased, a lowering of NEE occurred during spring and summer. This pattern is reversed during autumn and winter, for which increases in NEE can be seen as sea-ice area decreased and temperatures rose.

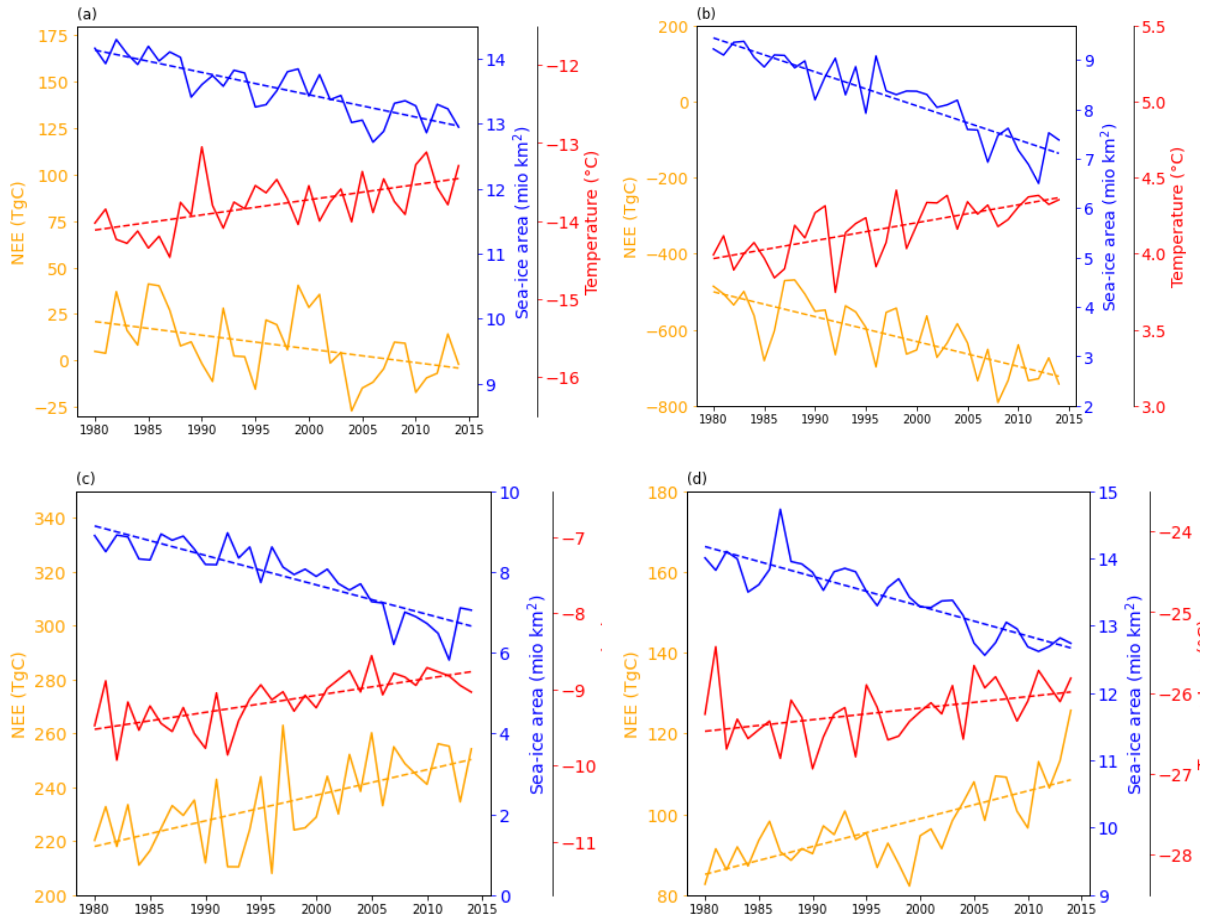

Figure 6. Pan-Arctic Trends of total sea-ice area, temperature and NEE in a) spring, b) summer, c) autumn and d) winter. Note that scales for each variable differ among plots, specifically for NEE in summer.

Figure 7 shows trends in sea-ice area, temperature and GPP on the left versus trends of sea-ice area, temperature and R_{eco} to the right.
The trends in sea-ice area and temperature are repeated from *Figure 5* for comparison.

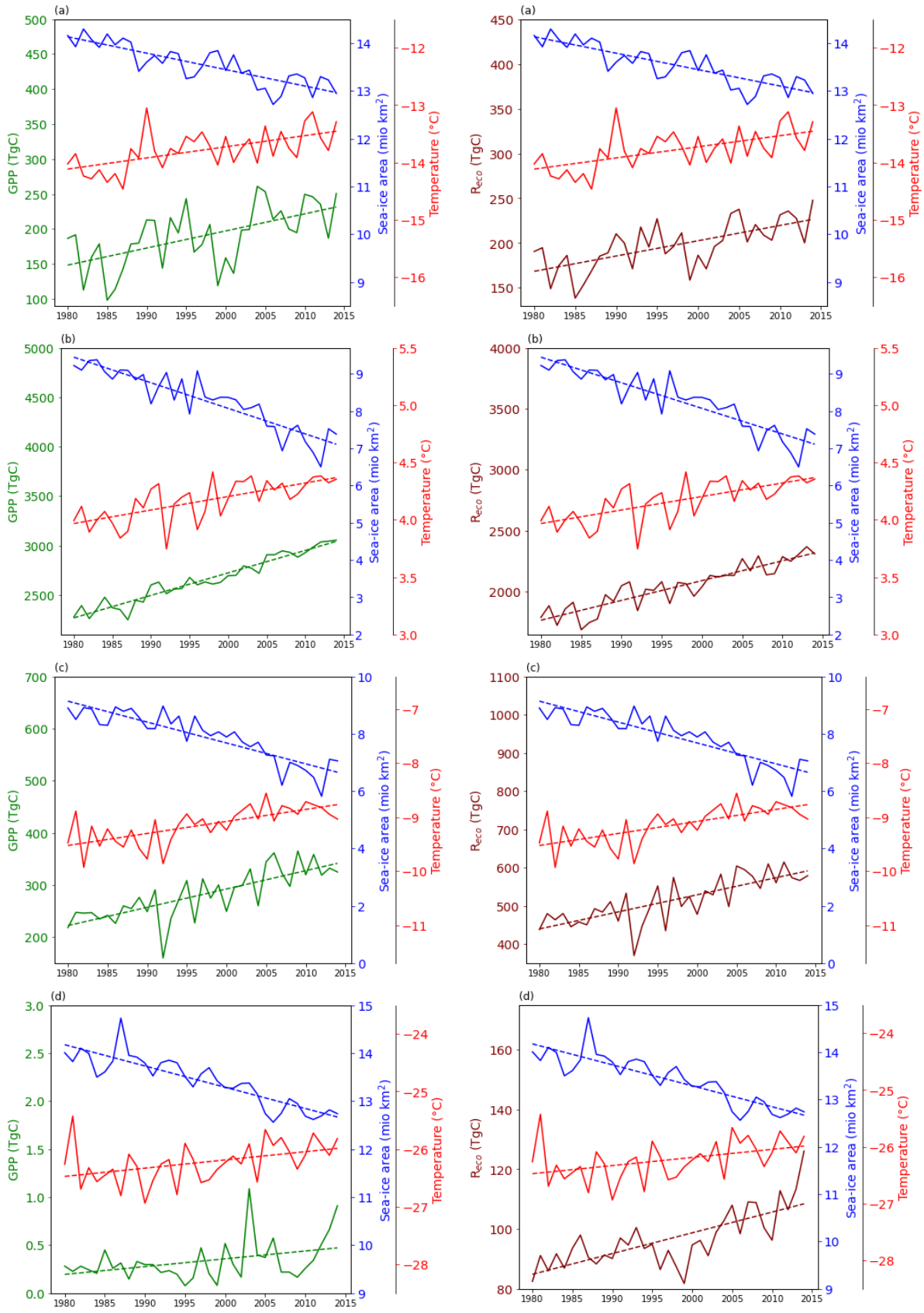

Figure 7. Times series of sea-ice area, temperature and GPP to the left versus time series of sea-ice area, temperature and ecosystem respiration (R_{eco}) to the right. Significant trends are

plotted for all variables. From top to bottom, panel a) shows spring trends, b) summer trends, c) autumn trends and panel d) winter trends

3.2 Correlations among detrended variables

Relationships between the detrended variables sea ice, temperature and the carbon fluxes are summarized in *Table 4* below, where Pearson correlation coefficients (R-values) represent the strength of the correlation. Non-significant relationships are denoted by NS.

Table 4. Pearson correlation coefficients r for the relationships between sea-ice area and carbon fluxes, and for temperature with carbon fluxes. Non-significant correlations (p >0.05, r <0.34) are denoted as NS. Significant p-values are denoted with asterisks (p<0.05, p<0.01**, p<0.001***)*

SPRING	*Sea Ice*	*Temperature*
Temperature	-0.37 *	-
GPP	-0.51 **	0.57 ***
NEE	0.53 **	-0.45 **
RH	-0.43 **	0.65
RA	-0.49 **	0.61

SUMMER	*Sea Ice*	*Temperature*
Temperature	-0.43 **	-
GPP	-0.54 **	0.49 **
NEE	NS	0.49 **
RH	-0.40 *	0.78 ***
RA	-0.48 **	0.58 ***

AUTUMN	*Sea Ice*	*Temperature*
Temperature	NS	-
GPP	-0.39 *	0.48 **
NEE	-0.35 **	0.55 ***
RH	-0.39 *	0.59 ***
RA	-0.45 **	0.47 **

WINTER	*Sea Ice*	*Temperature*
Temperature	-0.45 *	-
GPP	NS	NS
NEE	NS	NS
RH	NS	0.37 *
RA	NS	NS

A significant negative correlation was found between sea-ice area and GPP. This relationship is strongest for summer ($r = -0.54$, $p<0.05$), followed by spring ($r = -0.51$, $p<0.05$) and autumn ($r = -0.39$, $p<0.05$), whilst for winter no significant correlation was found.

Significant negative correlations existed between RA and sea-ice area for spring, summer and autumn. The relationship between RH and sea-ice area was of similar strength and of the same direction. No relationship could be found for winter sea-ice area with RA and RH.

A significant relationship between NEE and sea-ice area could only be found for spring, where this relationship is positive ($r = 0.53$, $p<0.05$) and for autumn ($r = -0.35$, $p<0.05$), where it is negative.

GPP correlated significantly and positively with temperature during spring ($r = 0.57$, $p <0.05$), summer ($r = 0.49$, $p<0.05$) and autumn ($r = 0.48$, $p<0.05$). No significant relationship could be found for winter. This is similar for RA, which also correlated positively with temperature, except for winter. This relationship was strong in spring ($r = 0.61$, $p<0.05$) and summer ($r = 0.58$, $p<0.05$) and moderate in autumn ($r = 0.47$, $p<0.05$).
RH showed a similar pattern, although generally less strong correlations with temperature and a significant (positive), although weak, relationship in winter ($r = 0.37$, $p<0.05$), opposed to RA and GPP. These correlations are as expected since the temperature data is used as input of LPJ-GUESS. Interestingly, they are not that different from the correlations to the independent sea-ice satellite data.

Opposed to the positive correlations between GPP, RA and RH with temperature, the direction of the relationship between NEE and temperature differs between the seasons. A significant negative relationship was found for spring (as temperature increased, NEE became more negative), whilst significant positive relationships were found for summer and autumn (as temperature increased, NEE became more positive).
The strongest relationship existed for autumn ($r = 0.55$, $p<0.05$), whereas for winter, again, no significant relationship could be found.

Temperature and sea-ice area correlated less strongly but always negatively. This relationship was significant during spring, summer and winter, where winter had the strongest relationship ($r = -0.45$, $p<0.05$). The lack of a correlation to sea ice in autumn is interesting. This is the time of year that sea ice reaches its minimum and the sea-ice albedo effect is strongest.

4 Discussion

4.1 Main findings

4.1.1 **Totals of carbon exchanged**

Total numbers in NEE per season reflect the increasing carbon sink of tundra over 1980-2014 and the observed greening trends from satellites (Bhatt et al., 2017). During spring, the values of NEE fluctuated around zero. Neither GPP, nor respiration dominated, however with a warming Arctic and sea-ice decline, GPP appears to be the dominant carbon flux. The fluctuations around zero for spring show the interannual variability, potentially resulting from changes (advancing) of the start of the growing season, as the trend towards negative NEE suggests. This trend towards carbon uptake in spring contributed to the annual lowering of NEE.

Summer NEE was consistently negative. This relatively strong carbon sink is the result of an increased GPP during the growing season compared to autumn and winter GPP, as a result of higher amounts of incoming solar radiation and warmer temperatures. Autumn NEE, in contrast to summer NEE, was consistently positive as a result of light limitation reducing GPP and making respiration the dominating flux. Continuous positive numbers in winter NEE were reported, although closer to zero than during autumn. This is the result of the lowering of all fluxes during winter, as a result of darkness and very low temperatures, reducing not only GPP

but also RA. RH becomes similarly reduced due to the low temperatures inhibiting CO_2 release from tundra soils. These seasonal variations found in NEE are supported by Bruhwiler et al. (2021), who found NEE to be negative during May - September and positive during October – April.

RH was found to make up a larger part of R_{eco} than RA. The proportional contribution of RA to R_{eco}, however, was found to have increased during spring and summer, since GPP increases strongly in these seasons which also raises RA. Hicks Pries et al. (2015) found that tundra RA in Healy (Alaska, 63.86°N) and Abisko (Sweden, 68.35°N) responded more strongly to warming and thawing of permafrost than RH during the growing season. However, their study uses observational data and a comparison to such data can not be made without a thorough analysis of the processes that caused their results and whether these are modelled in our data.
Segal and Sullivan (2014) reason that the observed increases in RA coupled to the increase of permafrost thaw during the warming season, opens up space for substrate availability and thus leads to the increase in both, RA and RH. It would be interesting to investigate this further in a future study.

Our finding of a negative tundra NEE indicate that the increased growing season losses from RA and old soil RH are compensated by GPP and agree with the findings by Hicks Pries et al. (2015) who reported similar results from flux measurements.

4.1.2 **Trends**

Trends in temperature, sea-ice area, GPP and respiration are, as expected, similar to previous research (Bhatt et al., 2017, Box et al. 2019, Bruhwiler et al. 2021, Parmentier et al. 2013). This indicates that tundra productivity and soil respiration increased as temperature rose, and sea ice declined.

One of our most important findings is a negative trend in NEE between 1980 and 2014, which is the opposite of what we expected to see. We therefore reject our second hypothesis of NEE becoming more positive with increasing temperatures as a result of a stronger carbon release than uptake.

The negative trends in NEE during spring and summer show that GPP increased more than respiration. This shows that even though respiration increased with a rise in temperatures, GPP became more dominant during spring and summer.
During autumn and winter, on the other hand, respiration was an increasing stronger flux, giving a positive trend in NEE. This can be explained by the fact that photosynthesis is light-limited and ceases when days become shorter in autumn towards polar night in winter, while respiration can continue to increase throughout the year with higher temperatures, which was previously posed by Parmentier et al. (2013).

4.1.3 **Correlations**

We expected to find a significant negative relationship between sea-ice area and GPP, as well as between sea-ice area and respiration. We found that sea-ice area and GPP correlated negatively, meaning that as sea ice declined, GPP increased. The negative correlations between RA and sea-ice area and between RH and sea-ice area, confirm that the higher productivity raised respiration in both plants and in the soil. Post et al. (2013) found that coastal tundra NDVI increased as sea ice declined, supporting our findings of GPP increasing with sea-ice decline. The lack of a correlations to the winter fluxes could be due to the carbon fluxes being small and

showing little variation. Our third hypothesis can be accepted, as sea-ice area between 1980 and 2014 did correlate significantly and negatively with GPP, RH and RA.

The relationship of sea-ice area with GPP was found to be strongest in summer, closely followed by spring. This could be due to the effect that the lowering of sea-surface albedo through sea-ice decline has on the absorption of incoming solar radiation during spring and summer in coastal areas. This causes more warming in the near-coastal tundra (Parmentier et al., 2013), allowing for increases in GPP. Temperatures are highest and sea-ice area the most reduced during the summer and autumn months (see *Figure 5*). However, even though autumn is warmer than spring, light is limiting GPP, whereas spring has enough light but lacks warmth, accounting for weaker correlations in spring and autumn compared to summer, where light availability is high enough to melt the ice and can cause the most warming.

RA and RH similarly increased as sea ice declined, possibly due to the above explained effects of a lower sea-surface albedo and warmer temperatures. Respiration seems to have been influenced even more by temperature than GPP. GPP was expected to have been affected less by temperature in autumn and winter than respiration, due to light limitation. The correlations indicate that this was indeed the case. During autumn RH was affected more by temperature than GPP, RA however was similarly less affected by temperature, as it is a fraction of GPP. During winter, RH is the only variable correlating significantly with temperature, probably due to the limited plant activity, affecting GPP and RA.

The increases in GPP, RA and RH during all seasons, except for winter, can be explained by the increase in temperature, when the variables of carbon exchange correlate well with temperature during these seasons. The stronger correlation of GPP during spring compared to summer and autumn can be explained by the lengthening of the growing season, i.e., as temperatures rise, the annual period with sufficient temperatures to allow photosynthesis, increases. Indeed, temperature increases between 1980-2014 were stronger for spring compared to summer. Out of GPP, RA and RH, the strongest correlation with temperature had RH during all seasons, as a result of the explained independence on light compared to GPP and RA, which was limited through GPP.

NEE correlated positively with sea-ice area during spring and negatively during autumn, which indicates a decrease in NEE (negative values) through the dominating sink in GPP in spring and an increase in NEE through the dominating respiration in winter. However, no significant correlation was found for the summer months, which is unexpected, since the carbon fluxes GPP, RA and RH all correlated well with sea-ice area during that time. This non-significant correlation of NEE with sea-ice area could be due to the opposite sign of GPP and R_{eco}, which means that they partly cancel each other out in the calculation of NEE. A change in NEE is therefore less apparent, even though GPP and respiration did change.

The varying direction of the relationship between NEE and temperature over the year is caused by the prior discussed variations in GPP and respiration being affected differently over the seasons. However, finding a positive relationship between summer NEE and temperature is unexpected and the opposite of what we can see from the trends, where NEE decreases during summer together with increasing temperatures. If this correlation is correct, this may indicate drought years, where GPP was reduced as a result of soil moisture limitation. This shows that the correlation between temperature and NEE may be different for the interannual variability compared to long term trends, but this would require further investigation, e.g., through scatter

plots of the correlations. Further analysis is needed to investigate the reasons behind this relationship, but this was omitted due to time limitations for this study.
Oddly enough, temperature and sea-ice area showed no significant relationship in the autumn. As Screen et al. (2012) report, autumn and early winter is when sea-ice decline has its strongest warming effect above the ocean. A reason for this missing correlation could be that the domain is too large. For example, near-land temperatures in areas such as Siberia could be less affected by heat transport from southern latitudes than near-land temperatures in Greenland or Norway. By averaging over the entire Arctic, the correlation is lowered and becomes insignificant. A regional analysis as done in Parmentier et al. (2015) would be more suitable to capture the spatial variations in the relation of the variables.
To summarize: Even though respiration could increase during all seasons, while GPP was limited to spring, summer and autumn, GPP increased at a higher rate than respiration (see *Figure 3*). This explains the negative trend in NEE, where higher uptake of carbon through photosynthesis (GPP) compared to carbon respired by plants and the soil is indicated by negative values for NEE.

4.2 Limitations

The main limitation of this study is the impossibility to say anything about the direction of influence between sea ice and temperature. Although our findings support the notion that sea-ice decline induced the changes on tundra carbon cycling via temperature, one has to be aware that the direction of influence between sea-ice decline and temperature is not only one directional. Temperature changes contribute to sea-ice decline, and this further warms the Arctic, forming a feedback mechanism. Sources of inaccuracies in the methodology and what could be improved are the spatially varying influence of sea ice on tundra, the mask and the statistical analysis.

4.2.1 **Sea-ice data**

Restrictions in the sea-ice data arise from the sensor resolution, the temporal coverage and algorithm assumptions. Weather effects along with mixing of ocean and land area captured by the sensors also contribute to some residual error (Comiso 2017). This dataset, however, is widely used and can be assumed to be reliable enough for this type of study. Small inaccuracies are assumed not to have had a significant effect on the outcomes of the study.
Since ice melt close to the land has a larger potential to affect tundra a more advanced spatial analysis would be necessary as proposed earlier.
Furthermore, we did not use the 15% threshold in sea-ice area, which is usually used. This should have improved the accuracy of the total sea-ice area. Including all cells containing sea ice (cells with less than 15% concentration) affects the results in giving higher numbers of total sea-ice area. Changes in sea-ice area are also more detailed which could have improved the correlations as all changes are included. It could, on the other hand, also have reduced the correlations due to changes that are not close to the ice edge and have less of an influence on tundra. In order to evaluate this, a more advanced spatial approach such as used by Parmentier et al. (2015) would be needed.

4.2.2 **LPJ-GUESS**

As with every other model, general uncertainties exist in the data, since a model can only represent part of the real world. However, LPJ-GUESS is a widely used and well performing vegetation model. The version used to generate the carbon fluxes used for this study uses an updated snow-scheme which improves its performance in modelling cold season processes, permafrost and carbon flux estimations, as well as improving soil carbon content simulations

which enables a better assessment of plant responses to future conditions during winter and reduces model uncertainties (Pongracz et al., 2021). This snow-scheme has a higher precision in modelling carbon exchanges in a warming Arctic compared to the single layer snow-scheme previously used in LPJ-GUESS. This is likely to enhance the accuracy of our data compared to earlier assessments using LPJ-GUESS.
Higher winter respiration and overall higher tundra carbon content result from this model improvement and could explain higher values compare to other people's work. McGuire et al. (2012), for example, found arctic tundra to be a sink of carbon (negative NEE) over 1990-2006 of an average of -214 $Tgyr^{-1}$ using LPJ-G WHyMe. This study finds the average annual carbon sink of tundra between 1980-2014 to have been -272 $TgCyr^{-1}$. This difference could be the result of the updated snow scheme.

No significant correlations were found for winter except for temperature with sea-ice area and RH, which could be the result of the very small winter fluxes and small changes in the other fluxes.
Bhatt et al. (2017) point out the need to consider atmospheric moisture from sea-ice melt as an indirect contributor to plant productivity through its influence on cloud cover and precipitation. A study by Buchwahl et al. (2020) raises the concern that the with sea-ice decline associated reduction in soil moisture (when evaporation outpaces precipitation) may inhibit the increase in shrub productivity that is aided by the warming. This version of LPJ-GUESS does not account for the changes in sea ice and atmospheric moisture feedbacks from the land (e.g. plants) directly (Zhang et al., 2020). The increases in GPP and respiration may be weaker as soil moisture reductions prevent the warming enhanced productivity. The result may be a weaker sink. Therefore, it would be interesting to investigate the carbon balance with this factor incorporated in the modelling.
To enable the modelling of these interactions, and thus a possibly more precise carbon balance under sea-ice decline, LPJ-GUESS should be run in a coupled mode, as an Earth system model, where in addition to the modelled vegetation dynamics through LPJ-GUESS, sea ice dynamics are accounted for as well, or in a regional climate model, a model that can show the feedback that vegetation change has on sea-ice decline as well (Zhang et al., 2020).

4.2.3 **Mask**
Inaccuracies may result from the applied mask. This mask is not a perfect representation of tundra locations and could be an overestimation in total tundra area. Therefore, fluxes may be slightly larger than in reality, however, this should not be a large difference.

4.2.4 **Correlations and significance**
Correlation is not causality. However, other papers (e.g., Bhatt et al. (2017)) support our results that sea ice has an effect on the carbon cycling of tundra through temperature and therefore the correlations can be seen as plausible. Since we cannot tell much about the direction of influence between temperature and sea-ice decline, the observed changes in tundra productivity can not be attributed to one of the variables alone. They are a combination of the interactions between sea-ice decline and a warming Arctic. The correlations with temperature were slightly stronger which supports that opposed to sea ice, the link between temperature and the carbon fluxes is direct, whilst changes in sea ice influence carbon cycling likely through temperature and moisture.

5 Conclusions

Our analysis only considered the carbon cycling of arctic tundra. To make assessments on the carbon budget of the Arctic, many more variables have to be taken into account. As proposed Earth System Models can be used to account for the atmospheric feedback of sea-ice decline. Even though this assessment can aid with providing knowledge on how tundra acted as a carbon sink under sea-ice decline and climate warming during 1980-2014, this study can not make assessments on the future state of tundra. Based on our findings and future projected warming (IPCC) it is very likely that sea ice will further decline and impact the carbon cycling of tundra, possibly in a similar pattern as reported here. This leads to the thinking that tundra will slow down global warming in taking up more carbon than under colder conditions. An assessment using observational data by Bruhwiler et al. (2021) revealed that the Arctic acted as CO_2 sink, but as a CH_4 source. However, with permafrost thaw a large release in CO_2 and CH_4 is expected, and if this happens it may reverse the increasing sink that observations and models have been showing over the past decades. The key findings are as follows:

- The annual NEE in the tundra region of the Northern Hemisphere was found to have been negative throughout the years 1980-2015, with a negative trend, agreeing that the carbon sink of tundra through GPP was stronger than the source of carbon through respiration and that this sink increased more than the source.

- The CO_2 flux of GPP increased between 1980-1989 and 2005-2014 by 762 TgC y^{-1}, CO_2 from respiration increased by 605 TgC y^{-1}. NEE decreased by 157 TgC y-1.

- Seasonal variations were found: Summer tundra was a strong carbon sink, spring trends went towards a sink, whilst for the remaining seasons respiration became more dominant.

- GPP was less affected by temperature in autumn and winter than respiration, due to light limitation.

- Sea-ice area and GPP and RA and RH correlated significantly and negatively, meaning that as sea ice declined, GPP, RA and RH increased.

- NEE correlated positively with sea-ice area during summer and negatively during autumn, which indicates a decrease in NEE through the dominating sink flux in GPP in summer and an increase in NEE through the dominating flux of respiration in winter.

We conclude that the warming of the Arctic influenced the carbon cycling of tundra, and that sea-ice decline plays likely a role therein. This facilitated the carbon sink through GPP more than the carbon source via respiration.

6 References

Bhatt, U. S., Walker, D. A., Raynolds, M. K., Bieniek, P. A., Epstein, H. E., Comiso, J. C., Pinzon, J. E., Tucker, C. J., Steele, M., Ermold, W., & Zhang, J. L. (2017). Changing seasonality of panarctic tundra vegetation in relationship to climatic variables. *Environmental Research Letters*, *12*(5). https://doi.org/ARTN 05500310.1088/1748-9326/aa6b0b

Box, J. E., Colgan, W. T., Christensen, T. R., Schmidt, N. M., Lund, M., Parmentier, F. J. W., Brown, R., Bhatt, U. S., Euskirchen, E. S., Romanovsky, V. E., Walsh, J. E., Overland, J. E., Wang, M. Y., Corell, R. W., Meier, W. N., Wouters, B., Mernild, S., Mard, J., Pawlak, J., & Olsen, M. S. (2019). Key indicators of Arctic climate change: 1971-2017. *Environmental Research Letters*, *14*(4). https://doi.org/ARTN 045010 10.1088/1748-9326/aafc1b

Bruhwiler, L., Parmentier, F. J. W., Crill, P., Leonard, M., & Palmer, P. I. (2021). The Arctic Carbon Cycle and Its Response to Changing Climate. *Current Climate Change Reports*, *7*(1), 14-34. https://doi.org/10.1007/s40641-020-00169-5

Buchwal, A., Sullivan, P. F., Macias-Fauria, M., Post, E., Myers-Smith, I. H., Stroeve, J. C., Blok, D., Tape, K. D., Forbes, B. C., & Ropars, P. (2020). Divergence of Arctic shrub growth associated with sea ice decline. *Proceedings of the National Academy of Sciences*, *117*(52), 33334-33344.

Demura, T., & Ye, Z.-H. (2010). Regulation of plant biomass production. *Current opinion in plant biology*, *13*(3), 298-303.

Harris, C. R., Millman, K. J., Van Der Walt, S. J., Gommers, R., Virtanen, P., Cournapeau, D., Wieser, E., Taylor, J., Berg, S., & Smith, N. J. (2020). Array programming with NumPy. *Nature*, *585*(7825), 357-362.

Hoyer, S., & Hamman, J. (2017). xarray: ND labeled arrays and datasets in Python. *Journal of Open Research Software*, *5*(1).

McKinney, W. (2010). Data structures for statistical computing in python. Proceedings of the 9th Python in Science Conference,

McKinney, W. (2015). Pandas, python data analysis library. *URL http://pandas. pydata. org*.

Meier, W. N., Serreze, M. C., & Stroeve, J. C. (2008). *Frequently Asked Questions on Arctic sea ice*. NSIDC. Retrieved May 19th from https://nsidc.org/arcticseaicenews/faq/#sunspots

Moon, T. A., M.L. Druckenmiller, and R.L. Thoman. (2021). *Arctic Report Card 2021*.

Parmentier, F.-J. W., Christensen, T. R., Sørensen, L. L., Rysgaard, S., McGuire, A. D., Miller, P. A., & Walker, D. A. (2013). The impact of lower sea-ice extent on Arctic greenhouse-gas exchange. *Nature climate change*, *3*(3), 195-202.

Polyakov, I. V., Walsh, J. E., & Kwok, R. (2012). Recent changes of Arctic multiyear sea ice coverage and the likely causes. *Bulletin of the American Meteorological Society*, *93*(2), 145-151.

Pongracz, A., Warlind, D., Miller, P. A., & Parmentier, F. J. W. (2021). Model simulations of arctic biogeochemistry and permafrost extent are highly sensitive to the implemented snow scheme in LPJ-GUESS. *Biogeosciences*, *18*(20), 5767-5787. https://doi.org/10.5194/bg-18-5767-2021

Screen, J. A., Deser, C., & Simmonds, I. (2012). Local and remote controls on observed Arctic warming. *Geophysical Research Letters*, *39*. https://doi.org/Artn L10709 10.1029/2012gl051598

Smith, B. (2001). LPJ-GUESS-an ecosystem modelling framework. *Department of Physical Geography and Ecosystems Analysis, INES, Sölvegatan*, *12*, 22362.

Smith, B., Prentice, I. C., & Sykes, M. T. (2001). Representation of vegetation dynamics in the modelling of terrestrial ecosystems: comparing two contrasting approaches within European climate space. *Global Ecology and Biogeography*, *10*(6), 621-637. https://doi.org/DOI 10.1046/j.1466-822X.2001.t01-1-00256.x

Smith, B., Warlind, D., Arneth, A., Hickler, T., Leadley, P., Siltberg, J., & Zaehle, S. (2014). Implications of incorporating N cycling and N limitations on primary production in an individual-based dynamic vegetation model. *Biogeosciences*, *11*(7), 2027-2054. https://doi.org/10.5194/bg-11-2027-2014

Viovy, N. (2018). CRUNCEP version 7-atmospheric forcing data for the community land model. *Research Data Archive at the National Center for Atmospheric Research, Computational and Information Systems Laboratory*, *10*.

Virkkala, A. M., Aalto, J., Rogers, B. M., Tagesson, T., Treat, C. C., Natali, S. M., Watts, J. D., Potter, S., Lehtonen, A., & Mauritz, M. (2021). Statistical upscaling of ecosystem CO2 fluxes across the terrestrial tundra and boreal domain: Regional patterns and uncertainties. *Global Change Biology*, *27*(17), 4040-4059.

Zhang, W., Döscher, R., Koenigk, T., Miller, P., Jansson, C., Samuelsson, P., Wu, M., & Smith, B. (2020). The interplay of recent vegetation and sea ice dynamics—results from a regional Earth system model over the Arctic. *Geophysical Research Letters*, *47*(6), e2019GL085982.